All-optical clock recovery from 10-Gb/s NRZ data and NRZ to RZ format conversion

Lina Yin (尹丽娜), Yumei Yan (闫玉梅), Yunfeng Zhou (周云峰), Jian Wu (伍 剑), and Jintong Lin (林金桐)

Key Laboratory of Optical Communication and Lightwave Technologies of MOE, Beijing University of Posts and Telecommunications, Beijing 100876

Received April 7, 2005

A non-return-to-zero (NRZ) to pseudo-return-to-zero (PRZ) converter consisting of a semiconductor optical amplifier (SOA) and an arrayed waveguide grating (AWG) is proposed, by which the enhancement of clock frequency component and clock-to-data suppression ratio of the NRZ data are evidently achieved. All-optical clock recovery from NRZ data at 10 Gb/s is successfully demonstrated with the proposed NRZ-to-PRZ converter and a mode-locked SOA fiber laser. Furthermore, NRZ-to-RZ format conversion of 10 Gb/s is realized by using the recovered clock as the control light of terahertz optical asymmetric demultiplexer (TOAD), which further proves that the proposed clock recovery scheme is applicable.

OCIS codes: 060.2360, 060.2330, 200.3050, 230.1150.

All-optical clock recovery is one of the most important functions for future all-optical communication networks. Many papers demonstrate clock recovery based on return-to-zero (RZ) format data[1,2]. However, the non-return-to-zero (NRZ) format data are actually widely used in current lightwave systems due to its better bandwidth efficiency. Clock recovery from NRZ format data is known to be rather difficult to implement due to the absence of discretely separated clock frequency component in its modulation spectrum. Therefore, for clock recovery from NRZ data, two stages are required, as shown in Fig. 1. First, a NRZ to pseudo-retrun-to-zero (PRZ) converter is used to realize clock component extraction from the NRZ data stream. Generally, an additional optical nonlinear element[3−7], such as a semiconductor optical amplifier (SOA), an optical interferometer or a SOA loop mirror, is required to realize conversion from NRZ data signal to PRZ signal which contains stronger clock components. Second, a clock recovery circuit is chosen to accomplish clock recovery from the converted PRZ signal. In this stage, the schemes applied for clock recovery from RZ data can be adopted, such as self-pulsating semiconductor laser or mode-locked fiber laser etc..

This paper demonstrates all-optical clock recovery from 10-Gb/s NRZ data signal, using the combination of a SOA and an arrayed waveguide grating (AWG) as clock component extractor and an injection mode-locked SOA fiber laser as clock recovery circuit. Moreover, the recovered clock is applied as a control signal of a terahertz optical asymmetric demultiplexer (TOAD) to realize format conversion from NRZ to RZ, which testified its practical applicability.

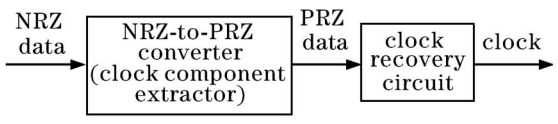

Fig. 1. Schematic of clock recovery from NRZ data.

In order to derive a clock frequency component from the original NRZ data, this paper proposes a NRZ-to-PRZ converter including a SOA and an AWG, whose principle is shown in Fig. 2. When the optical NRZ data with wavelength λ enter into the SOA, the wavelength near the leading edge of the NRZ data is red-chirped to $\lambda + \Delta\lambda$ due to the self-phase modulation (SPM) occurring as the result of index nonlinearity induced by gain saturation of the SOA. At the same time, an overshoot is generated at the leading edge of the NRZ data, which contains a stronger clock frequency component, however, the suppression ratio between the clock frequency component and the modulation component is very low because the NRZ modulation signal component still exists within the output signal of the SOA[3,4], therefore, further processing is usually required. In this paper, an AWG is introduced in order to obtain a signal with higher clock-to-data suppression ratio. The center wavelength of the output channel of AWG is set near $\lambda + \Delta\lambda$ to obtain the red-chirped wavelength components and to filter out other wavelengths containing data components. In this way, the PRZ signal with higher clock-to-data suppression ratio is generated at every leading edge of NRZ data, which is beneficial for clock recovery. After the clock-enhanced PRZ signal is injected into the clock recovery circuit such as a mode-locked SOA fiber laser, clock pulse trains will be generated due to cross gain modulation (XGM) of SOA when the mode-locking condition is satisfied. The proposed NRZ-to-PRZ converter is simple, stable, and nearly polarization insensitive. In

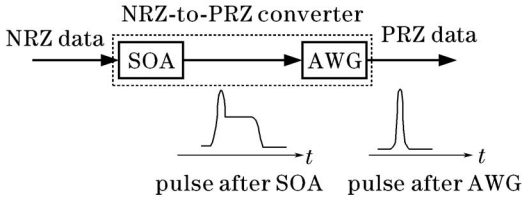

Fig. 2. NRZ-to-PRZ converter.

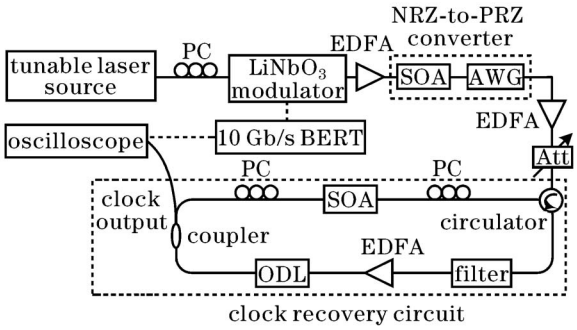

Fig. 3. Experimental setup of clock recovery from NRZ data (Att: optical attenuator).

particular, the combination of SOA and AWG provides a potential method for multi-wavelength clock recovery in future wavelength division multiplexing (WDM) networks.

Figure 3 shows the experimental setup of clock recovery from NRZ data. The NRZ data is produced using a tunable continuous wave (CW) laser source (HP8168F), whose operating wavelength is set at 1548.13 nm, modulated by a $LiNbO_3$ modulator driven by a bit error rate tester (BERT) at 10 Gb/s. The PRZ signal is generated from the above-mentioned NRZ-to-PRZ converter consisting of a SOA (IPSAD1501) and an AWG (JDS Uniphase MA40X1LCSPC000). The central wavelength of the output channel of AWG is selected as 1549.32 nm with 3-dB bandwidth of 0.4 nm. Before injected into the mode-locked SOA fiber laser, the PRZ data signals firstly pass through an erbium-doped fiber amplifier (EDFA) and an optical attenuator in order to control the input data power applied to modulate the SOA in the cavity. In experiment, the average power of the PRZ data sequence injected into the laser cavity is about 11 dBm. The clock recovery circuit adopts a simple injection mode-locked SOA fiber laser, including a SOA, a tunable optical filter, a variable optical delay line (ODL), two polarization controllers (PCs), and a coupler. SOA is a key element for clock recovery, which corresponds to a gain medium and a modulator to provide gain and gain modulation in the cavity. The SOA exhibits 0.5-dB polarization gain dependence, so two PCs are used for performance optimization. A circulator is used for introducing the PRZ data into the cavity. A tunable optical filter is used for selecting wavelength of clock pulses and a coupler is used for clock output. The pulse waveform and the radio-frequency (RF) spectrum are displayed by using a digital sampling oscilloscope (Tektronix 11801C). The optical spectrum is measured by using an optical spectrum analyzer (ANDO AQ6315B) with a resolution of 0.05 nm. In order to obtain clock pulses at the expected repetition rate, the variable ODL is precisely adjusted for matching of the data modulation rate to the fundamental frequency of the fiber ring laser. The recovered clock pulses are wavelength tunable and very stable, which can work for several hours continuously without special stable method owning to the nearly polarization independence of SOA.

Figure 4 shows the experimental results of clock recovery from a fixed data sequence 1001011101011100 at 10 Gb/s. Figures 4(a), (b), (c), and (d) show the waveforms of the input NRZ data, the data after SOA, the converted PRZ data (the data after AWG), and the recovered

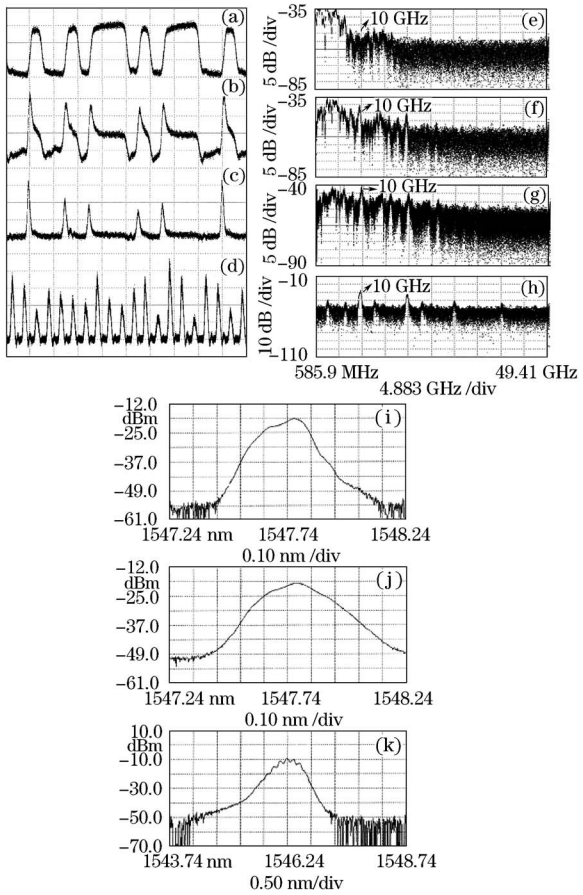

Fig. 4. Clock recovery from a fixed data sequence 1001011101011100 at 10 Gb/s. Waveforms of the input NRZ data (a), the data after SOA (b), the converted PRZ data (c), and the recovered clock (d); RF spectra of the input NRZ data (e), the data after SOA (f), the converted PRZ data (g), and the recovered clock (h); optical spectra of the input NRZ data (i), the data after SOA (j), and the recovered clock (k).

clock at 10 GHz, respectively. Figures 4(e), (f), (g), and (h) show the corresponding RF spectra of the input NRZ data, the data after SOA, the converted PRZ data, and the recovered clock, respectively. As can be seen in Fig. 4(e), there is almost no discretely separated clock frequency component at 10 GHz in the input NRZ data. After passing through the SOA, an overshoot is generated at the leading edge of the NRZ data shown in Fig. 4(b), meanwhile, the clock frequency component at 10 GHz of the data is enhanced by about 10 dB (in Fig. 4(f)) compared to that of the original NRZ data, however other frequency components are still rather strong and the clock-to-data suppression ratio is still low. After passing through the AWG, the PRZ data are generated (in Fig. 4(c)), the data component is attenuated by 5 dB and the clock frequency component almost has no change (in Fig.4(g)), so the clock-to-data suppression ratio is again increased by about 5 dB. Therefore, by using the NRZ-to-PRZ converter, the clock frequency component is enhanced by 10 dB and the clock-to-data suppression ratio is improved by about 15 dB owning to the enhanced clock frequency components and the attenuated data components, which is beneficial for further clock recovery. By injecting the converted NRZ data into the mode-locked fiber laser, the recovered clock will be

achieved, as shown in Fig. 4(d). The amplitudes of the converted PRZ data in Fig. 4(c) and the recovered clock in Fig. 4(d) are uneven owning to the pattern effect of the SOA, which can be reduced by a CW assist light[8]. Figures 4(i), (j), and (k) show the optical spectra of the input NRZ data, the data after SOA, and the recovered clock at 10 GHz, respectively. As shown in Fig. 4(i), there is almost no discretely separated spectral line in the optical spectrum of the input NRZ data and the 3-dB bandwidth of the spectrum is about 0.122 nm. After the NRZ data entering into the SOA, the 3-dB bandwidth of its optical spectrum is extended to 0.168 nm (in Fig. 4(j)), at the same time, strong red-chirped wavelength components containing a stronger clock frequency component at 10 GHz are generated owning to SPM effect, which can be further filtered by AWG. As for the optical spectrum of the recovered clock in Fig. 4(k), clearly split spectral lines spaced by 10 GHz are generated, which indicate that the clock pulses are achieved ideally.

Figure 5 shows the experimental results of clock recovery from $2^{15}-1$ PRBS NRZ data at 10 Gb/s. Figures 5(a), (b), (c), and (d) show the waveforms of the input NRZ data, the data after SOA, the converted PRZ data, and the recovered clock, respectively. The waveform

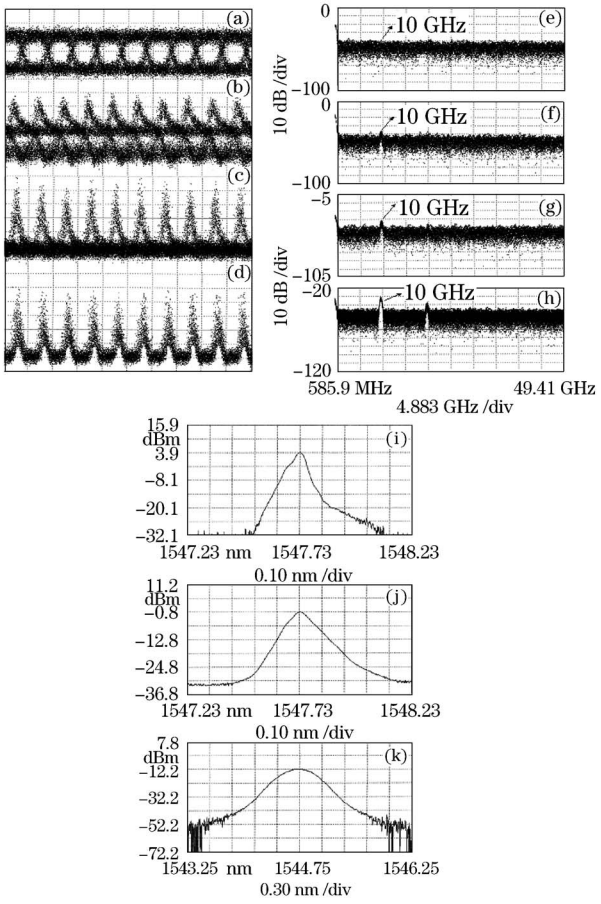

Fig. 5. Clock recovery from $2^{15}-1$ PRBS NRZ data at 10 Gb/s. Waveforms of the input NRZ data (a), the data after SOA (b), the converted PRZ data (c), and the recovered clock (d); RF spectra of the input NRZ data (e), the data after SOA (f), the converted PRZ data (g), and the recovered clock (h); optical spectra of the input NRZ data (i), the data after SOA (j), and the recovered clock (k).

of the recovered clock in Fig. 5(d) is not very clear mainly because the input NRZ data in Fig.5(a) contain a rather high noise caused by the poor performance of the $LiNbO_3$ modulator, besides the pattern effect caused by the longer carrier lifetime of SOA. Figures 5(e), (f), (g), and (h) show the corresponding RF spectra of the input NRZ data, the data after SOA, the converted PRZ data, and the recovered clock, respectively. The discretely separated clock frequency component at 10 GHz is nearly absent in the NRZ data shown in Fig. 5(e). When the NRZ data pass through the SOA, the clock frequency component at 10 GHz is enhanced by about 5 dB (in Fig. 5(f)). Furthermore, after the data passing through AWG, the data component is attenuated by 5 dB and the clock frequency component at 10 GHz almost has no change (in Fig. 5(g)), so the clock-to-data suppression ratio is again increased by about 5 dB. Therefore, compared with the input NRZ data, more than 5 dB clock enhancement and 10 dB clock-to-data suppression ratio enhancement of the PRZ data are realized with the proposed NRZ-to-PRZ converter. Figures 5(i), (j), and (k) show the optical spectra of the input NRZ data, the data after SOA, and the recovered clock, respectively. These optical spectra clearly indicate that the 3-dB bandwidth of the optical spectrum is extended from the original 0.048 nm for the NRZ data (in Fig. 5(i)) to 0.075 nm for the data after SOA (in Fig. 5(j)), meanwhile, the generation of red-chirped wavelength components implies the enhancement of clock frequency component. The optical spectrum in Fig. 5(k) has no clearly split spectral lines spaced by 10 GHz mainly because of the poor performance of the recovered clock, which can be improved by using a $LiNbO_3$ modulator with good performance to generate the NRZ data.

Format conversion is one of the key technologies for the future optical networks[9]. By using the above experimental results of clock recovery, NRZ to RZ format conversion is further realized based on TOAD[10]. The principle can be explained in Fig. 6. The NRZ data is injected into TOAD through port A as a probe light, whose input power is too weak to cause nonlinearity of SOA. Whereas the clock pulses at the same bit rate with the NRZ data are injected into port B as a control light, whose input power is strong enough to induce a phase change of SOA, so a periodical switching window will generate in TOAD. If the NRZ data and the clock are synchronized with each other, when the NRZ data is "1", TOAD will output a RZ bit "1", when the NRZ data is "0", TOAD will output a RZ bit "0". In this way, NRZ to RZ format conversion will be realized.

Figure 7 shows the experimental results of NRZ to RZ format conversion. The input NRZ data are the fixed data sequence 1001011101011100 at 10 Gb/s. Figures

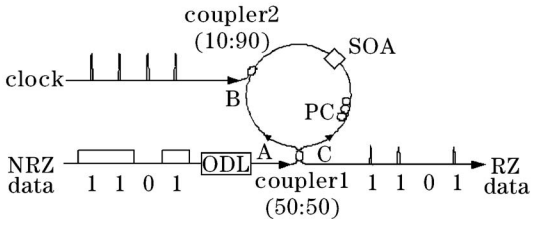

Fig. 6. NRZ-to-RZ format conversion based on TOAD.

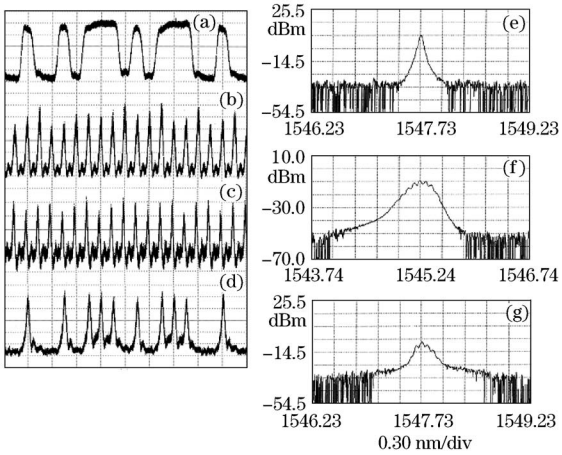

Fig. 7. NRZ-to-RZ format conversion. Waveforms of the input NRZ data (a), the recovered clock (b), TOAD's switching window (c), and the converted RZ data (d); optical spectra of the NRZ data (e), the recovered clock (f), and the converted RZ data (g).

7(a), (b), (c), and (d) show the waveforms of the original NRZ data, the recovered clock, TOAD's switching window, and the converted RZ data. As can be seen in these figures, there is no evident pattern effect in the converted RZ data (in Fig. 7(d)) and its extinction ratio is about 10 dB. Figures 7(e), (f), and (g) show the optical spectra of the original NRZ data, the recovered clock, and the converted RZ data, respectively. As shown in these figures, the original NRZ data (in Fig. 7(e)) has no split spectrum line, whereas in the converted RZ data (in Fig. 7(g)), evident spectral lines are generated spaced by 10 GHz (the spectrum interval is 0.08 nm). The experimental results of format conversion demonstrate better the applicability of the proposed scheme.

In conclusion, this paper proposes a NRZ-to-PRZ converter consisting of a SOA and an AWG. Using the proposed converter, the clock-to-data suppression ratios of the $2^{15}-1$ PRBS NRZ data and a fixed data sequence 1001011101011100 at 10 Gb/s are enhanced more than 10 and 15 dB, respectively, which is beneficial for further clock recovery. In experiment, all-optical clock recovery from NRZ data at 10 Gb/s is successfully realized with this converter and a mode-locked SOA fiber laser. Furthermore, format conversion from NRZ to RZ is realized by using a TOAD, in which the recovered clock is used as the control light of TOAD, emphasizing the practical applicability of the proposed clock recovery scheme for NRZ data. The extinction ratio of the converted RZ data is about 10 dB. The schemes for clock recovery from NRZ data and NRZ-to-RZ format conversion will be useful for high-speed all-optical communication networks.

This work was supported by the National Natural Science Foundation of China (No. 90401025), and Key Project of MOE (No. 105036). L. Yin's e-mail address is yinlina_bupt@163.com.

References

1. Y. Li and G. Li, Electron. Lett. **38,** 892 (2002).
2. K. Vlachos, G. Theophilopoulos, A. Hatziefremidis, and H. Avramopoulos, IEEE Photon. Technol. Lett. **12,** 705 (2000).
3. H. J. Lee, H. G. Kim, J. Y. Choi, and H. K. Lee, Electron. Lett. **35,** 989 (1999).
4. W. Mao, M. Al-Mumin, X. Wang, and G. Li, IEEE Photon. Technol. Lett. **13,** 239 (2001).
5. H. K. Lee, J. T. Ahn, M.-Y. Jeon, K. H. Kim, D. S. Lim, and C. H. Lee, IEEE Photon. Technol. Lett. **11,** 730 (1999).
6. W. Hong and D. Huang, Acta Opt. Sin. (in Chinese) **24,** 781 (2004).
7. M. Yao, H. Tang, M. Fukazawa, J. Zhou, K. Vahala, M. Newkirk, and B. Miker, in *Proceedings of OFC96*, pp.177—178 (1996).
8. L. Yin, G. Liu, J. Wu, and J. Lin, Proc. SPIE **5625,** 86 (2004).
9. L. Xu, B. C. Wang, V. Baby, I. Glesk, and P. R. Prucnal, IEEE Photon. Technol. Lett. **15,** 308 (2003).
10. M. Eiselt, W. Pieper, and H. G. Weber, J. Lightwave Technol. **13,** 2099 (1995).